RainFARM: Rainfall Downscaling by a Filtered Autoregressive Model

NICOLA REBORA AND LUCA FERRARIS

Centro di Ricerca Interuniversitario in Monitoraggio Ambientale, University of Genoa, Savona, Italy

JOST VON HARDENBERG AND ANTONELLO PROVENZALE

Istituto di Scienze dell'Atmosfera e del Clima, CNR, Torino, and Centro di Ricerca Interuniversitario in Monitoraggio Ambientale, University of Genoa, Savona, Italy

(Manuscript received 26 May 2005, in final form 7 November 2005)

ABSTRACT

A method is introduced for stochastic rainfall downscaling that can be easily applied to the precipitation forecasts provided by meteorological models. Our approach, called the Rainfall Filtered Autoregressive Model (RainFARM), is based on the nonlinear transformation of a Gaussian random field, and it conserves the information present in the rainfall fields at larger scales. The procedure is tested on two radar-measured intense rainfall events, one at midlatitude and the other in the Tropics, and it is shown that the synthetic fields generated by RainFARM have small-scale statistical properties that are consistent with those of the measured precipitation fields. The application of the disaggregation procedure to an example meteorological forecast illustrates how the method can be implemented in operational practice.

1. Introduction

Rainfall prediction on scales of the order of a few kilometers in space and less than an hour in time is a necessary ingredient to issue reliable flood alerts in small catchments, such as those found in mountain and urban environments and along the Mediterranean coast.

Effective precipitation forecasts are typically obtained from limited-area meteorological models (LAMs) that include both the synoptic conditions provided by general circulation models (GCMs), into which they are nested, and the mesoscale processes that are active on regional scales (e.g., Pielke 1984).[1] An issue of concern is that LAM rainfall estimates are not reliable on small scales, owing to the incomplete numerical representation of small-scale processes and to the limited resolution of the observational network used for initialization and data assimilation. Nonhydrostatic numerical models also display strong sensitivity to the choice of parameterization schemes and to numerical resolution (Adlerman and Drogemeier 2002). For these reasons, the skill of operational rainfall prediction becomes poor at spatial scales of a few tens of kilometers, even though the nominal resolution of nonhydrostatic LAMs can be less than 5 km. As a consequence, rainfall predictions are currently not reliable on the scales needed for flood forecast in small Mediterranean-type basins with areas of a few hundred square kilometers (Ferraris et al. 2002).

One way to tackle this issue is to use stochastic downscaling (or disaggregation) techniques to generate small-scale ensemble rainfall predictions (Ferraris et al. 2002). Downscaling models aim at generating an ensemble of stochastic realizations of the small-scale precipitation fields that have statistical properties similar to those measured for rainfall in a given area and/or synoptic situation. Because a downscaled precipitation field is the product of a stochastic process, it cannot be taken as a faithful deterministic prediction of small-scale precipitation, but rather as one realization of a process with the appropriate statistical properties. That is, a downscaling procedure does not provide "the" future of the system, but rather an ensemble of realistic

[1] Limited-area models solve the equations of motion for the moist atmosphere in a limited spatial domain with a typical size of a few thousands kilometers, and have a resolution of a few kilometers. Some of the older LAMs are based on the hydrostatic approximation, while modern nonhydrostatic LAMs can resolve part of the spectrum of atmospheric convection. LAMs used in operational practice are usually nested into hydrostatic general circulation models, which integrate the atmospheric equations on the whole sphere or in one hemisphere. LAMs should not be confused with cloud resolving models, which explicitly resolve moist convection and some of the active microphysical processes, include advanced turbulent closures, but can currently simulate much smaller domains than LAMs.

Corresponding author address: Nicola Rebora, Centro di Ricerca Interuniversitario in Monitoraggio Ambientale, University of Genoa, Via Cadorna 7, I-17100 Savona, Italy.
E-mail: nicola@cima.unige.it

possible futures. It is essential to repeat the downscaling procedure several times and generate an ensemble of downscaled fields to be used in rainfall-runoff models to produce the corresponding ensemble of basin responses. From these, one can estimate the probability of a flood event and the related uncertainty (Siccardi et al. 2004).

In past years, several rainfall downscaling algorithms have been proposed. With some simplification, the different approaches can be grouped into three main families: (i) point processes based on the random positioning of a given number of rainbands and rain cells (Waymire et al. 1984; Rodriguez-Iturbe et al. 1986; Eagleson et al. 1987; Northrop 1998; Wheater et al. 2000; Willems 2001; Cowpertwait et al. 2002), (ii) autoregressive processes passed through a static nonlinear transformation (Mejia and Rodriguez-Iturbe 1974; Bell 1987; Guillot and Lebel 1999; Lanza 2000), sometimes called "meta-Gaussian" models, and (iii) fractal cascades (Lovejoy and Mandelbrot 1985; Schertzer and Lovejoy 1987; Gupta and Waymire 1993; Davis et al. 1994; Over and Gupta 1996; Perica and Foufoula-Georgiou 1996; Menabde et al. 1997a,b, 1999; Deidda et al. 1999; Deidda 2000). Mixed models, combining the above approaches, have also been developed (Veneziano et al. 1996; Veneziano and Iacobellis 2002). In fact, despite significant differences in their construction, all of the model classes mentioned above are able to reproduce the main statistical properties of rainfall, including anomalous scaling (von Hardenberg et al. 2000; Ferraris et al. 2003a,b). Thus, the choice between them should be dictated by their ability to be nested into meteorological forecasts, preserving the large-scale information and propagating it to small scales.

From an operational point of view, a downscaling algorithm must in fact be able to derive the small-scale statistical properties of rainfall from the properties of a (forecasted or measured) precipitation field defined on larger scales. Following this approach, in this work we introduce a downscaling procedure based on nonlinearly filtering the output of a linear autoregressive process, whose properties are derived from the information available on larger scales. The model discussed here is easily nested into large-scale rainfall predictions, and it uses simple statistical properties of the large-scale fields (viz., the shape of the power spectrum) to downscale the information provided by meteorological models. Since the procedure is developed for operating on the outputs of limited-area meteorological models, the resolved scales are typically those of mesoscale structures, that is, they are a few tens of kilometers in space and a few hours in time, and the fields are downscaled to about 1 km in space and a few minutes in time.

The rest of this paper is organized as follows. The downscaling approach is further discussed in section 2. The model adopted here, called the Rainfall Filtered Autoregressive Model (RainFARM), is described in section 3. To illustrate the working of the RainFARM procedure and to test its performance, in section 4 we apply the method to two intense rainfall events measured by meteorological radars. In section 5 we apply the RainFARM method to the output of a limited-area model at midlatitudes. Section 6 is devoted to discussion and conclusions.

2. Modeling rainfall by a filtered autoregressive process

In the past 20 years, the analysis and simulation of rainfall fields has led to extensive knowledge of the small-scale statistical properties of rainfall. Different types of precipitation patterns (e.g., stratiform or convective, frontal or resulting from isolated thunderstorms, etc.) can significantly differ in their statistical properties. Many studies have focused on tropical convective precipitation, such as that measured during the Global Atmospheric Research Program (GARP) Atlantic Tropical Experiment (GATE) (Houze 1977; Houze and Betts 1981; Lovejoy and Mandelbrot 1985; Gupta and Waymire 1993; Over and Gupta 1994; Polyak and North 1995; Ferraris et al. 2003a) and the Tropical Ocean Global Atmosphere Coupled Ocean–Atmosphere Response Experiment (TOGA COARE) (Webster and Lukas 1992; Short et al. 1997; von Hardenberg et al. 2003; Deidda et al. 2004), while others have considered the properties of midlatitude precipitation patterns (e.g., Schiesser et al. 1995). Some of the main statistical features of intense rainfall fields at spatial scales between about 1 and 200 km and temporal scales between a few minutes and several hours are (Ferraris et al. 2003a,b)

- non-Gaussian probability distribution of rainfall intensity, both in space and time;
- spatial and temporal power spectral densities that grow with scale (i.e., so-called "red" spectra), with an approximate power-law behavior;
- approximate scaling (i.e., power law) behavior of the structure functions and of the partition functions of different order;
- anomalous scaling behavior (or multifractality), that is, different values of the scaling exponents and of the generalized fractal dimensions of different order;
- intermittency between rain/no-rain periods and areas; and

- the presence of intense rain cells with exponential profiles (von Hardenberg et al. 2003).

Rainfall downscaling models used to generate stochastic precipitation fields must be able to reproduce the statistical properties listed above. In this work we adopt a downscaling procedure based on the nonlinearly filtering of a linear autoregressive process, a type of approach discussed in detail by Bell (1987) and sometimes referred to as a "meta-Gaussian model" (Guillot and Lebel 1999). We found this model to be especially appropriate for nesting into measured or forecasted precipitation fields with coarse resolution and for downscaling the information they convey.

3. RainFARM

In the implementation of the downscaling procedure, we assume that we have access to a mesoscale rainfall field $P(X, Y, T)$, produced, for example, by a limited-area meteorological model. Here, X and Y indicate spatial coordinates and T indicates time. The field P is defined on the range of scales of $L_0 \le (X, Y) \le L_{\max}$ and $T_0 \le T \le T_{\max}$. The lower cutoff scales, L_0 and T_0, do not necessarily represent the nominal resolution of the field to be downscaled, but rather the scale below which the precipitation forecast becomes poor. Typically, $L_0 \approx$ 10–20 km and $T_0 \approx$ 2–4 h. The upper spatial and temporal scales $L_{\max}$ and $T_{\max}$ are determined by the size of the domain and the duration of the event. Hereafter, we use capital letters for quantities that are defined on scales larger than L_0 and T_0.

The goal of the disaggregation procedure is to generate a stochastic field $r(x, y, t)$, with spatial resolution $\lambda_0 < L_0$ (typically, $\lambda_0 \approx 1$ km) and temporal resolution $\tau_0 < T_0$ (typically, $\tau_0 \approx 10$ min), obtained by downscaling the statistical properties of the field P to small scales. The behavior of the downscaled field r for scales between L_0 and λ_0 and T_0 and τ_0 should represent one possible realization of the (unknown) small-scale behavior of the true precipitation field. We shall use lower-case letters for quantities that are defined on the whole range of scales from (λ_0, τ_0) to the regional scales $(L_{\max}, T_{\max})$. That is, the lower-case variables are defined on a range that includes (and extends to smaller scales) the range on which the upper-case variables are defined.

By aggregating the field r on spatial and temporal scales L_0 and T_0, we obtain a coarse-grained field $R(X, Y, T)$. A central requirement of the current procedure is that the aggregated field R should be equal to the original field P.

In detail, the RainFARM approach includes the following steps:

1) We estimate the space–time power spectrum $|\hat{P}(K_X, K_Y, \Omega)|^2$ of the field P. Here, K_X and K_Y are the wavenumbers in the X and Y directions and Ω is the angular frequency. Clearly, $(K_X, K_Y) \le \pi/L_0$ and $\Omega \le \pi/T_0$, where π/L_0 is the Nyquist wavenumber and π/T_0 is the Nyquist frequency of the field to be downscaled.
2) We extrapolate the power spectrum $|\hat{P}|^2$ to small scales. To do so, we assume the power spectrum of the rainfall field to have an approximate power-law behavior, consistent with the outcome of several analyses on the structure of precipitation fields (e.g., Ferraris et al. 2003a,b and references therein). From the original field, we estimate the spatial and temporal logarithmic slopes of the power spectrum $|\hat{P}|$, which we call α and β, respectively. For simplicity, we assume isotropy in the two spatial directions.
3) We generate a Fourier spectrum $\hat{g}(k_x, k_y, \omega)$ that ranges from $2\pi/L_{\max}$ to π/λ_0 in wavenumber and from $2\pi/T_{\max}$ to π/τ_0 in frequency, defined as

$$\hat{g}(k_x, k_y, \omega) = |\hat{g}(k_x, k_y, \omega)| \exp(i\phi), \tag{1}$$

where $\phi(k_x, k_y, \omega)$ are random, uniformly distributed phases. For the power spectrum, here we use the functional form

$$|\hat{g}(k_x, k_y, \omega)|^2 \propto (k_x^2 + k_y^2)^{-\alpha/2}\omega^{-\beta}. \tag{2}$$

By inverting the Fourier spectrum, we obtain a Gaussian field $g(x, y, t)$ defined on the whole range of scales $\lambda_0 \le (x, y) \le L_{\max}$, $\tau_0 \le t \le T_{\max}$, which we normalize to unit variance.
4) We generate a synthetic precipitation field $\tilde{r}(x, y, t)$ by taking a nonlinear transformation of the Gaussian field g. Here we use the simple transformation

$$\tilde{r}(x, y, t) = \exp[g(x, y, t)], \tag{3}$$

which leads to a lognormal field $\tilde{r}$.
5) We force the synthetic field to be equal to the original field P when aggregated on the scales (L_0, T_0). To this end, we define a coarse-grained synthetic field $\tilde{R}(X, Y, T)$ by aggregating the small-scale field $\tilde{r}$ on the scale (L_0, T_0), and we compute the ratio $P/\tilde{R}$ in each box with size (L_0, T_0). We then define a new synthetic field

$$r(x, y, t) = \tilde{r}(x, y, t)\frac{P(X, Y, T)}{\tilde{R}(X, Y, T)}, \tag{4}$$

such that $R = P$, where R is the field r aggregated on the scales (L_0, T_0). Here we use a top-hat aggregation (i.e., we integrate over boxes in space–time); other smoother forms of aggregation can be used as well.

When aggregated on space and time scales larger than L_0 and T_0, the field r behaves exactly as the original field P. The stochastic nature of the downscaled field r is manifest only on small scales, and it is associated with the choice of the set of random Fourier phases. The RainFARM approach is easily used for ensemble predictions; by choosing different sets of random Fourier phases, one can generate a large number of stochastic fields that are all equal to P when aggregated on space and time scales larger than L_0 and T_0, and are different, but with similar statistical properties, on smaller scales.[2]

In the above procedure, we have defined specific functional forms for the spectrum and the nonlinear transformation used on the range of scales that are unresolved by the original field. Other choices for these functional forms are of course possible, and they should be explored in specific applications.[3]

The stochastic field r produced by the RainFARM procedure has a non-Gaussian amplitude distribution, whose form is fixed by the specific nonlinear transformation adopted, and displays multifractal behavior. The version of the procedure described above has two free parameters, namely, the two spectral slopes in space and time α and β. These are determined from the estimates of the spectral slopes of the original field P, that is, without any prior knowledge of the small-scale behavior of the precipitation field.

Note that the RainFARM approach does not generate zero precipitation values in regions where the original precipitation field is nonzero. That is, wherever $P(X, Y, T) \neq 0$, the application of the downscaling procedure generates a small-scale field r that can be very small, but nevertheless strictly positive. To generate pixels with no precipitation in the downscaled field, one can introduce a small threshold r_0 (typically of the order of a few tenths of millimeters per hour for pixels with a size of the order of kilometers), such that the precipitation intensity is set to zero if the value r generated by the RainFARM is smaller than r_0. The value of the threshold is fixed, and it does not change with scale. In the following, we adopt this approach and, after the small-scale field is generated, we set to zero all of the spatiotemporal pixels with size (λ_0, τ_0), where $r < r_0$.

Before closing this section, some cautionary notes are in order. First, one could wonder whether a more general transformation, such as $\tilde{r} = \exp(bg)$, could be preferable. We experimented with such a family of transformations; in the examples discussed below the gain obtained by introducing this further degree of freedom is small, but the need for optimizing the new parameter b makes the whole procedure slower and more cumbersome. Thus, in operational applications we opted for using a simple exponential transformation.

The version of the model discussed here assumes spatial isotropic fields, a reasonable choice for the situations considered in this work. Other systems, such as squall lines, are highly anisotropic. In such cases, one should assume a different form of the power spectrum, where the logarithmic spectral slopes in the x and y directions are kept different. A similar approach was explored by Kumar and Foufoula-Georgiou (1993a,b) in the context of wavelet-based models.

A further point concerns the fact that we define the spectral slopes from the original field P, while we use them for generating a Gaussian field $\tilde{r}$. The form of the spectrum is not invariant under nonlinear transformations (e.g., Balmforth et al. 1999), and thus, in principle, the spectral slopes can change after the exponential transformation of $\tilde{r}$ is applied. However, the change in the spectral slopes resulting from the nonlinear transformation is much smaller than the uncertainty associated with the estimate of the spectral slopes from the large-scale portion of the spectrum, and this problem can be safely discarded.

An important issue concerns the scales of applicability of this model. From a mathematical point of view, any downscaling model can extend the large-scale spectral information to arbitrarily small scales. From a physical point of view, the extension is meaningful only when it is confined to the range of scales that are characterized by an approximate scaling behavior (i.e., by a well-defined shape of the power spectrum). A second requirement is that the information available on large scales is sufficient to determine the value of the spectral slopes. The above constraints imply that the use of a scaling-based stochastic downscaling model is meaningful in a range of spatial scales between about 50 and 1

[2] RainFARM works with a generic choice of the spatial–temporal combination L_0 and T_0, provided (a) that there is enough information at large scales to determine the spectral slopes and (b) it is meaningful to assume a scaling behavior for the spectrum. The choice of the specific couples of spatial and temporal scales used to start the downscaling procedure are dictated by the resolution of the data to be downscaled and by meteorological consistency; for example, it would be questionable to use a spatial scale of 100 km and a temporal scale of 1 min.

[3] In a recent work, Marani (2005) has shown that in many occasions one should not directly assume a power-law form of the moments of the amplitude distribution. In such cases, the same author showed that a power-law form of the autocorrelation, or equivalently of the power spectrum as we use here, often provides a good representation of the precipitation field. In some other cases, an exponential form of the autocorrelation can be preferred. Future developments of the downscaling procedure discussed here could include a choice between these two options.

km, and temporal scales between about 12 h and a few minutes.

4. Test of RainFARM on radar data

The best way to test the performance of a downscaling procedure is to start with a high-resolution (measured or simulated) precipitation field p and artificially degrade its resolution by coarse graining. This provides a smoother field P, which can be used as input to the downscaling model. The performance of the downscaling procedure can then be verified by assessing whether the reconstructed fields r reproduce the correct rainfall pattern and the statistical properties of the true field p.

To test the performance of the RainFARM procedure, we opted for using two datasets of high-resolution radar estimates of the precipitation field $p(x, y, t)$, which refer, respectively, to an intense rainfall event at midlatitudes and to intense convective precipitation over the tropical ocean.

a. Test 1: Intense precipitation at midlatitudes

The radar data considered here were measured by the C-band meteorological radar in San Pietro Capofiume (Bologna, Italy) managed by Agenzia Regionale Prevenzione e Ambiente (ARPA), Servizio Idro Meteorologico (SIM) Emilia Romagna. The event considered was measured on the 25 December 2001, starting at 0000 UTC. The event had a total duration of about 16 h and average rainfall intensity of 2.5 mm h^{-1} with peaks up to 115 mm h^{-1}. We selected this specific event because it is a typical example of intense fall/winter precipitation at midlatitudes and it includes both convective and stratiform parts. We analyzed other similar events measured by the same and other radars in Italy and found analogous results.

The duration of the precipitation record is $T_{max} = 16$ h and the radar measurements cover a square domain of side $L_{max} = 128$ km. The radar frames are recorded on a regular grid with a resolution $\lambda_0 = 1$ km. The time interval between different images is $\tau_0 = 15$ min. To test the downscaling procedure, the radar-estimated precipitation field $p(x, y, t)$ is aggregated to a resolution $L_0 = 8$ km in space and $T_0 = 1$ h in time, providing a coarse-grained field $P(X, Y, T)$ to be used as input to RainFARM. The downscaling procedure is then repeated, to generate an ensemble of 100 stochastic realizations of small-scale fields whose statistical properties are compared with those of the original field p.

First, we compare the average behavior of the original and RainFARM fields. Figure 1 shows the time evolution of the instantaneous spatial average of the original field p and of 100 RainFARM fields. An overall excellent agreement between the instantaneous spatial averages is observed.[4]

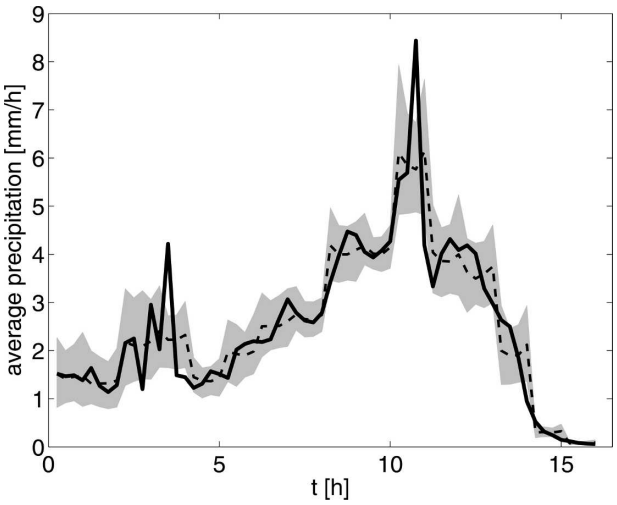

FIG. 1. Temporal evolution of the instantaneous spatial average of the original field p (solid line) and of an ensemble of 100 realizations of the stochastic field $r(x, y, t)$ produced by RainFARM for the midlatitude intense rainfall event discussed in the text. The dashed line indicates the average on the ensemble of stochastic realizations, and the shaded gray area includes 95% of the values of the individual fields.

The spatial and temporal power spectra of the original small-scale field p and an ensemble of 100 RainFARM fields r are shown in Fig. 2. For the event considered here, the spectra of the downscaled fields are in excellent agreement with the original spectra on the whole range of scales. Given that the spectra of the synthetic fields have been generated by a prescribed functional form whose parameters have been determined only from the large-scale spectral information, we think that the agreement between the spectra seen in Fig. 2 is quite impressive.

Next, we test how the different moments of the one-point probability distribution of precipitation intensity depend on scale. To this end, we aggregate the fields p and r in space and time on spatiotemporal volumes with size $\varepsilon = (\lambda, \tau)$, where $\lambda_0 \leq \lambda \leq L_{max}$ and $\tau_0 \leq \tau \leq T_{max}$. In particular, we aggregate on the scales (1 km, 0.25 h), (2 km, 0.5 h), (4 km, 1 h), (8 km, 2 h), (16 km, 4 h), and (32 km, 8 h). For this comparison, we include a small precipitation threshold $r_0 = 0.2$ mm h^{-1} at the smallest scale, so that for each pixel with size (λ_0, τ_0) we impose $r = 0$ if $r \leq r_0$. For each spatiotemporal aggregation

[4] The downscaling procedure conserves, by construction, the spatiotemporal average over the reliable scales L_0 and T_0, not the instantaneous spatial average of the fields. The agreement between the instantaneous spatial averages is thus a test of the goodness of the model.

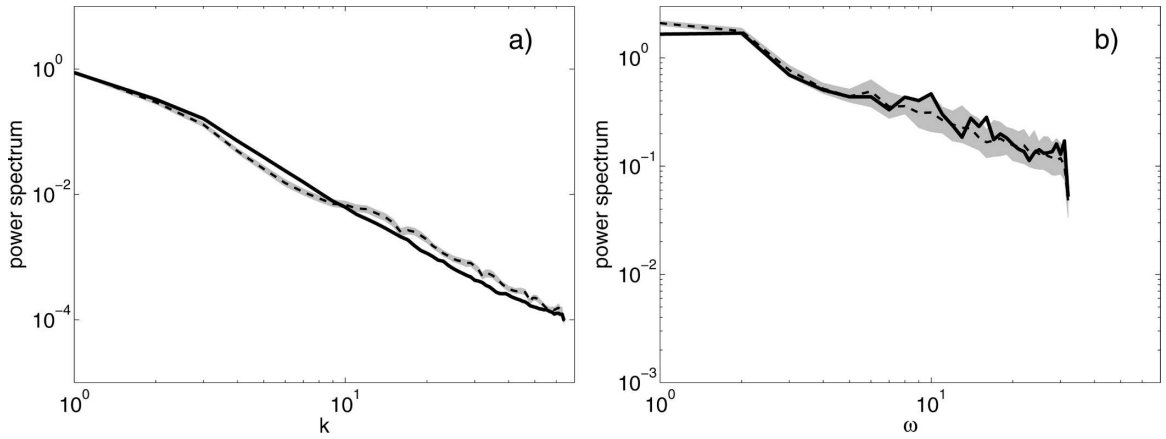

FIG. 2. (a) Spatial radial power spectrum, and (b) temporal power spectrum of the original field $p(x, y, t)$ and an ensemble of 100 realizations of the stochastic field $r(x, y, t)$ produced by RainFARM for the midlatitude intense rainfall event. Solid lines indicate the spectra of the original fields, dashed lines indicate the average spectra on the ensemble of stochastic realizations, and the shaded gray area includes 95% of the spectra of the downscaled fields.

scale we compute the variance, the skewness, and the kurtosis of the one-point probability distribution of the precipitation amplitude, and the number of regions (with size λ and τ) with zero precipitation. We do not consider the volume because this is imposed to be the same in the original and the downscaled fields.

Figure 3 shows these statistical moments as a function of the spatiotemporal aggregation scale (λ, τ). Note the excellent agreement in the values and the scale dependence of the statistical moments for the original and RainFARM fields.[5] These results indicate that the RainFARM procedure is capable of generating fields with the right behavior of the higher-order moments.

A final point concerns the reproduction of the anomalous scaling (multifractal) properties of the precipitation fields. We opted for estimating the generalized spatiotemporal partition functions $C_q(\varepsilon)$. To estimate them, we first introduce the measure $\mu_i(\varepsilon)$, defined as the integral of the field p in a spatiotemporal volume ε, with spatial side λ (on x and y) and temporal duration τ,

$$\mu_i(\varepsilon) = \frac{1}{V} \int_{x_i-\lambda/2}^{x_i+\lambda/2} dx \int_{y_i-\lambda/2}^{y_i+\lambda/2} dy \int_{t_i-\tau/2}^{t_i+\tau/2} dt\, p(x, y, t), \tag{5}$$

where (x_i, y_i, t_i) is the center of the ith spatiotemporal box with size (λ, τ) and V is the total rainfall volume over the event. The partition functions are defined as

$$C_q(\varepsilon) = \sum_i \mu_i(\varepsilon)^q, \tag{6}$$

where the sum is extended to all of the spatiotemporal boxes with size (λ, τ) and q is the order of the moment.

For a field with scaling properties, the partition functions exhibit a power-law dependence on scale, that is,

$$C_q(\varepsilon) \propto \varepsilon^{(q-1)D_q}. \tag{7}$$

The quantities D_q are the generalized fractal dimensions. Monofractal (or simple scaling) measures have $D_q = D_s$ for $q \neq s$, while multifractal measures (also said to display anomalous scaling) are characterized by $D_q > D_s$ for $q < s$.

It is instructive to consider first the case where no precipitation threshold is introduced, that is, $r_0 = 0$. Figures 4a and 4b show the generalized partition functions for $q = 0, 0.5, 1.5, 2, \ldots, 8$, for the original field and for one realization of the ensemble of RainFARM fields, respectively. Approximate scaling (i.e., approximate power-law dependence of the partition functions) is visible at least in a part of the scale range, and we can operationally define the "effective" generalized fractal dimensions by estimating the average slope of log C_q versus log ε in a preselected range of scales.[6] Figure 5a

[5] The statistical properties shown in Fig. 3 have been computed from the whole fields, including pixels with zero precipitation. One may wonder whether the good agreement between the statistical properties of the data and of the downscaled fields could be because of this choice. To address this question, we have computed the statistical properties of the fields considering only the pixels where precipitation is larger than zero, obtaining equivalent results.

[6] Much can be said about the presence or absence of scaling behavior in rainfall, and much has indeed been said. In this work, we are not interested in the issue of whether true scaling is present. Rather, we use the partition functions and the operational definition of the effective generalized dimensions as a statistical test to compare the properties of the original and stochastic fields.

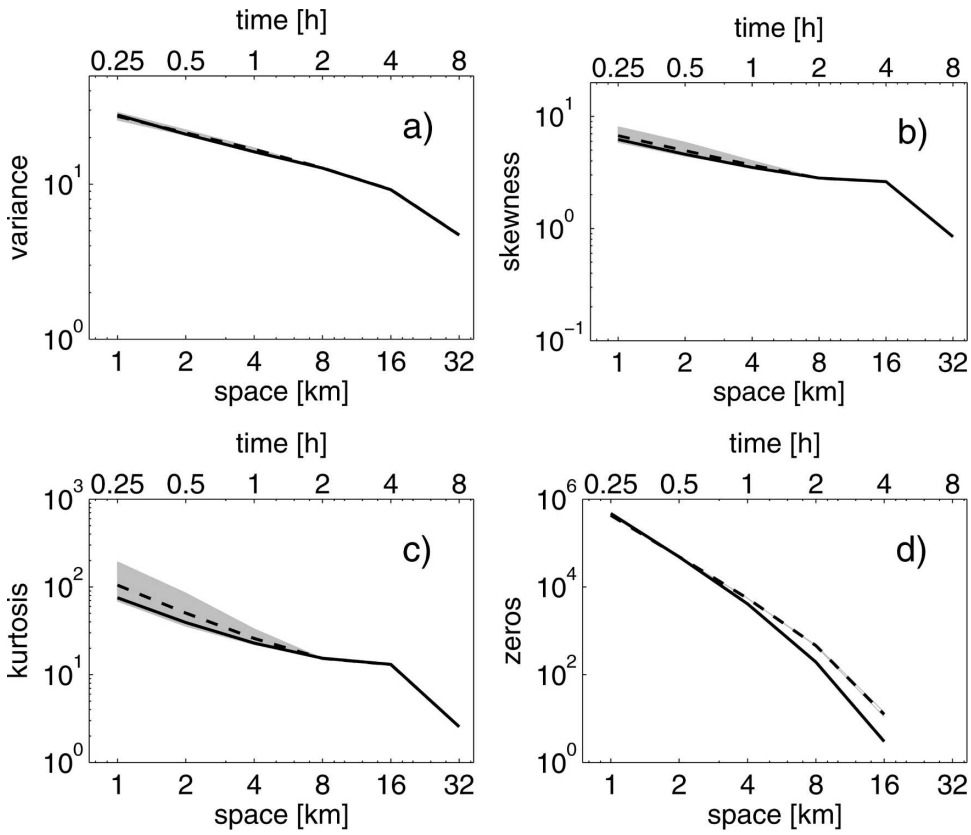

FIG. 3. Spatiotemporal scale dependence of the (a) variance, (b) skewness, (c) kurtosis, and (d) number of regions with zero precipitation for the original and for an ensemble of 100 realizations of RainFARM fields for the midlatitude intense rainfall event. A small threshold $r_0 = 0.2$ mm h^{-1} has been introduced at the smallest scales. Solid lines indicate the moments of the original fields, dashed lines indicate the average on the ensemble of stochastic realizations, and the shaded gray area includes 95% of the moments of the downscaled fields. Lower and upper horizontal scales indicate the spatial and temporal scales on which the average has been taken.

shows the effective generalized fractal dimensions D_q versus the order of the moment q for the original field p and for the downscaled fields. The generalized fractal dimensions have been computed from the average logarithmic slope of the partition functions on the scale range (2 km, 0.5 h)–(32 km, 8 h). The decrease of the values of the generalized dimensions for increasing moment order q indicates the presence of anomalous scaling behavior. A very good agreement between the generalized fractal dimensions of the original and the synthetic fields is visible for $q > 1$, indicating that the stochastic fields display an anomalous scaling behavior similar to that of the original field.

The disagreement in the generalized dimensions for $q < 1$ is because of the fact that the downscaled fields do not have, by construction, any pixel with strictly zero precipitation, other than those that are inside areas where $P = 0$. If we introduce the small precipitation threshold $r_0 = 0.2$ mm h^{-1}, so that for each pixel at the smallest scale (λ_0, τ_0) we impose $r = 0$ if $r \leq r_0$, we obtain the generalized dimensions reported in Fig. 5b, which now agree for the whole range of values of q.

In the RainFARM procedure, we found that the most delicate issue is the estimate of the spectral slopes from the original field P. An error in the estimated slopes can drastically alter the performance of the model. Special care should thus be used in estimating the spatial and temporal spectral slopes. These estimates become much harder when the original field is defined on a small range of scales. In the example considered here, the field to be downscaled is defined on scales ranging from $L_0 = 8$ km to $L_{\max} = 128$ km and from $T_0 = 1$ h to $T_{\max} = 16$ h, and a good estimate of the spectral slopes was possible.

b. *Test 2: Convective precipitation over the tropical ocean*

In this second test, we apply the RainFARM procedure to an intense convective precipitation event mea-

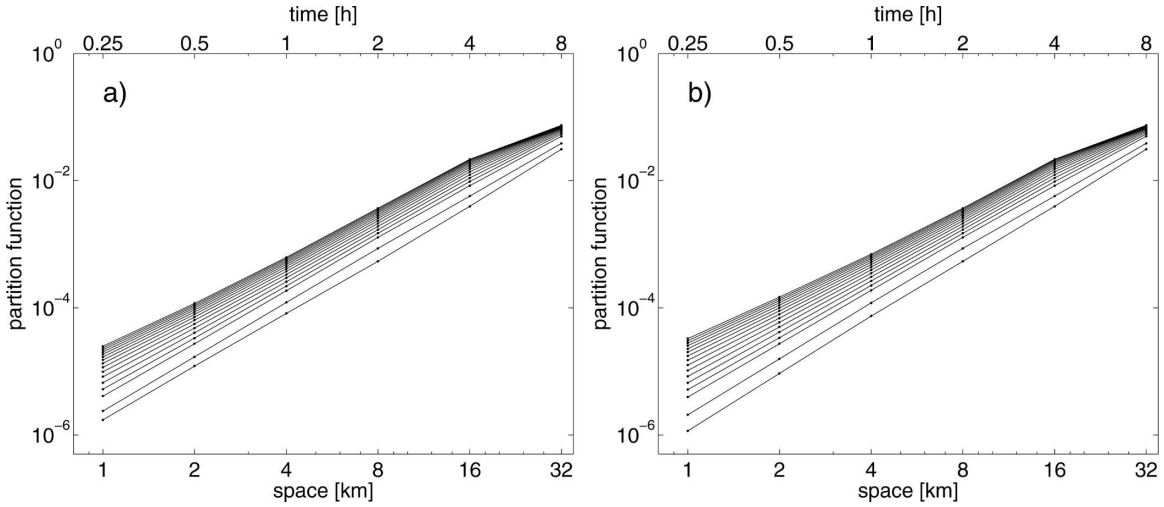

FIG. 4. Partition functions for (a) the original precipitation field and for (b) one realization of the ensemble of RainFARM fields for the midlatitude intense rainfall event. Lower and upper horizontal scales indicate the spatial and temporal scales on which the partition functions have been computed.

sured during TOGA COARE (Webster and Lukas 1992). The TOGA COARE fields are characterized by the presence of many convective precipitation cells with an approximately exponential shape (von Hardenberg et al. 2003), and they represent a well-studied example of tropical convective precipitation.

The TOGA COARE field $p(x, y, t)$ analyzed here is composed of 128 spatial records of precipitation intensity (mm h^{-1}), obtained from radar reflectivities, with a scan every 10 min and total record time from 2030 local time (LT) 28 December to 1750 LT 29 December 1992 (i.e., $T_{max} = 21$ h 20 min). The spatial resolution is 2 km and the field covers a square box with $L_{max} = 256$ km sides (Short et al. 1997). We degrade the resolution of $p(x, y, t)$ by aggregating the field on the spatial scale $L_0 = 8$ km and temporal scale $T_0 = 40$ min, obtaining a coarse-grained field $P(X, Y, T)$ that is then downscaled with the RainFARM procedure. In the following, we compare the statistical properties of the original field p with those of an ensemble of 100 downscaled fields r.

Figure 6 shows the time evolution of the instantaneous spatial average of the original field p and of the 100 downscaled fields. An excellent agreement is again

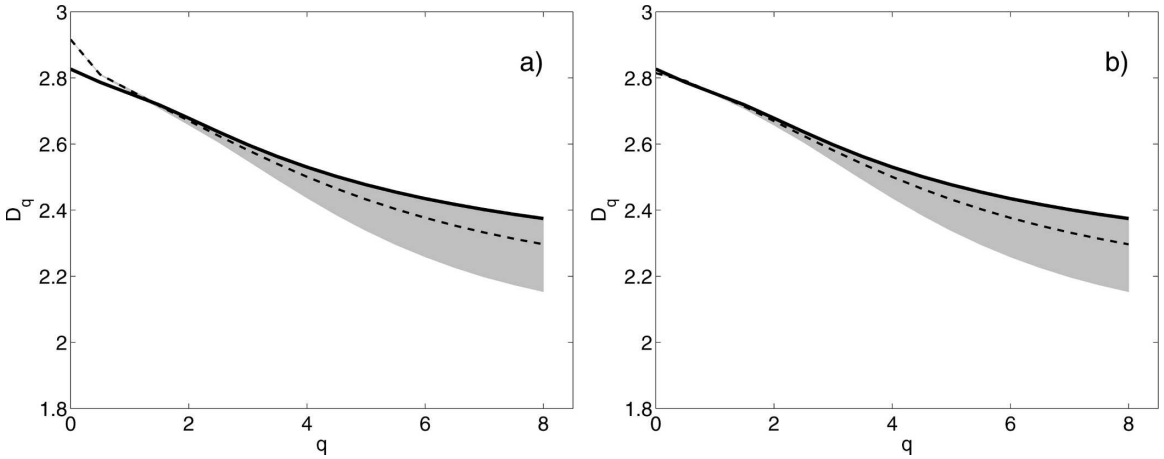

FIG. 5. Effective generalized fractal dimensions for the original field and for an ensemble of realizations of RainFARM for the midlatitude intense rainfall event. Solid lines indicate the generalized dimensions of the original field, dashed lines indicate the average on the ensemble of stochastic realizations, and the shaded gray area includes 95% of the dimensions of the downscaled fields. The generalized dimensions have been estimated from the average logarithmic slopes of the partition functions in the scale range from (2 km, 0.5 h) to (32 km, 8 h). (a) The raw RainFARM fields, and (b) the case where a small precipitation threshold has been included.

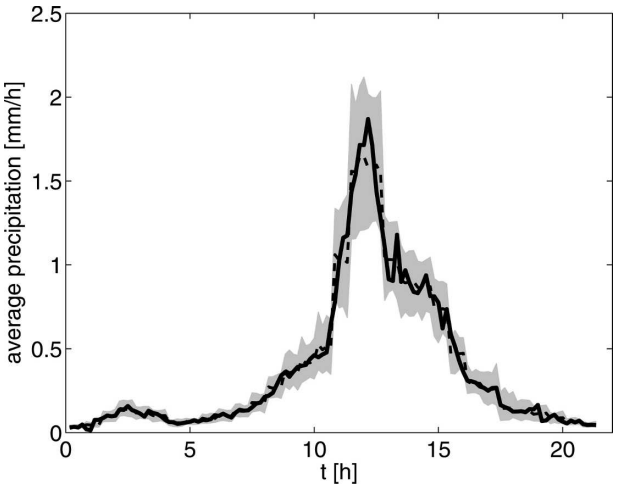

FIG. 6. Temporal evolution of the instantaneous spatial average of the original field p (solid line) and of an ensemble of 100 realizations of the stochastic field $r(x, y, t)$ produced by RainFARM for the TOGA COARE event discussed in the text. The dashed line indicates the average on the ensemble of stochastic realizations, and the shaded gray area includes 95% of the values of the individual fields.

found between the averages of the original and reconstructed fields.

Figure 7 shows the spatial and temporal power spectra of the original small-scale field p and of the ensemble of 100 downscaled fields r. In this case, the agreement between the original and downscaled fields is lower. This can be because of the fact that the spatial spectrum of the TOGA COARE data has less of a power-law shape than that of the midlatitude example and the temporal spectrum is much flatter. Both factors can affect the reconstruction of the missing information.[7]

Figure 8 shows the variance, skewness, kurtosis, and number of regions with zero precipitation for the original and RainFARM fields as a function of the aggregation scale. A small precipitation threshold $r_0 = 0.2$ mm h^{-1} has been included at the smallest scale. The fields p and r have been aggregated in space and time on spatiotemporal volumes with size $\varepsilon = (\lambda, \tau)$, where $\lambda_0 \leq \lambda \leq L_{\max}$ and $\tau_0 \leq \tau \leq T_{\max}$. In particular, here we aggregate on the scales (2 km, 10 min), (4 km, 20 min), (8 km, 40 min), (16 km, 80 min), (32 km, 160 min), and (64 km, 320 min). Note the good agreement in the values and the scale dependence of the skewness and kurtosis for the original and downscaled fields. The variance shows much larger differences, consistent with the difficulties encountered in reconstructing the power spectrum.

Figure 9 shows the effective generalized fractal dimensions D_q versus the order of the moment q for the original and RainFARM fields. The overall dependence of D_q on q is the same for the original and the downscaled fields, indicating the same type of multifractal behavior. However, there is a constant difference between the values of D_q of the TOGA COARE field and of the RainFARM fields, which is again consistent with the difficulty of properly estimating the spectral slope.

These results point again to the fact that the most delicate aspect of the whole procedure is the estimate of the spectral slopes from the large-scale portion of the spectrum. For example, if we impose in the procedure the correct average spectral slopes instead of using their estimates at larger scales, a much better agreement between the TOGA COARE and RainFARM statistics is obtained. However, in a true downscaling procedure we do not have access to the "right" slopes and we must thus be content with the estimates obtained from scales larger than L_0 and T_0.

5. Application of RainFARM to LAM precipitation forecasts

In this section we illustrate how the RainFARM procedure is applied to the precipitation forecast provided by a limited-area meteorological model.[8]

[7] These results, which hold also for other examples of midlatitude events and TOGA COARE data, suggest that midlatitude events have a clearer powerlaw spectral dependence and a steeper temporal spectral slope than tropical convective events. The current formulation of the RainFARM procedure is more appropriate for midlatitude precipitation.

[8] One may wonder whether a statistical downscaling approach applied directly to the output of a GCM could be preferable to the three-step procedure of GCM–LAM–downscaling adopted here. We are currently testing the applicability of RainFARM to the ensemble prediction system (EPS) produced by ECMWF and comparing the results with those obtained by downscaling the ensemble predictions obtained by nesting a nonhydrostatic mesoscale model in the GCM forecasts. In general, the intermediation of a nonhydrostatic LAM is supposed to not simply propagate the information and the bias of the CGM, but also to include dynamical processes that are not resolved by the GCM, such as orographic and/or convective precipitation. That is, a LAM is expected not only to redistribute precipitation (as the downscaling approach considered here does) but also to generate precipitation resulting from mesoscale processes that are not resolved by the GCM. In addition, the reliability scale of the GCM (more than 100 km) can be too large to justify the scaling assumption used to downscale the large-scale information.

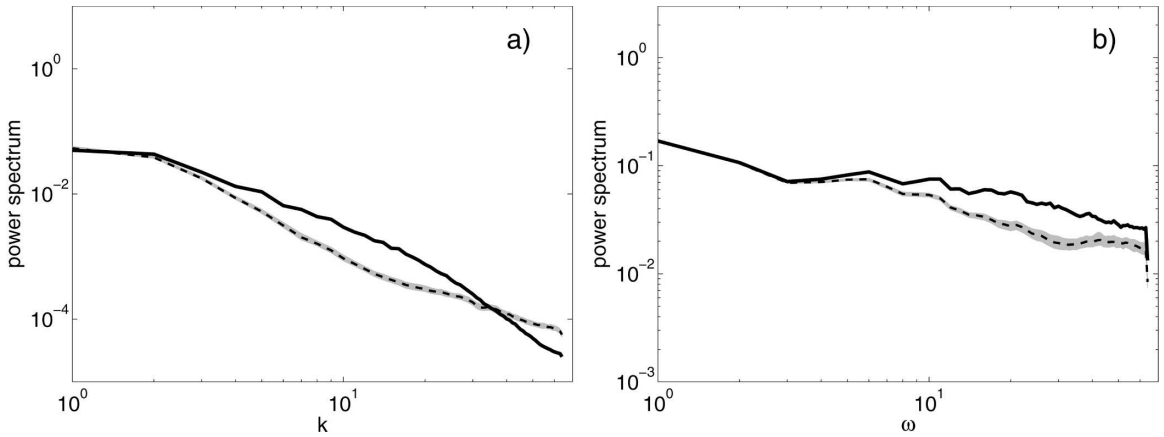

FIG. 7. (a) Spatial radial power spectrum and (b) temporal power spectrum of the original field $p(x, y, t)$ and of an ensemble of 100 realizations of the stochastic field $r(x, y, t)$ produced by RainFARM for the TOGA COARE event. Solid lines indicate the spectra of the original fields, dashed lines indicate the average spectra on the ensemble of stochastic realizations, and the shaded gray area includes 95% of the spectra of the downscaled fields.

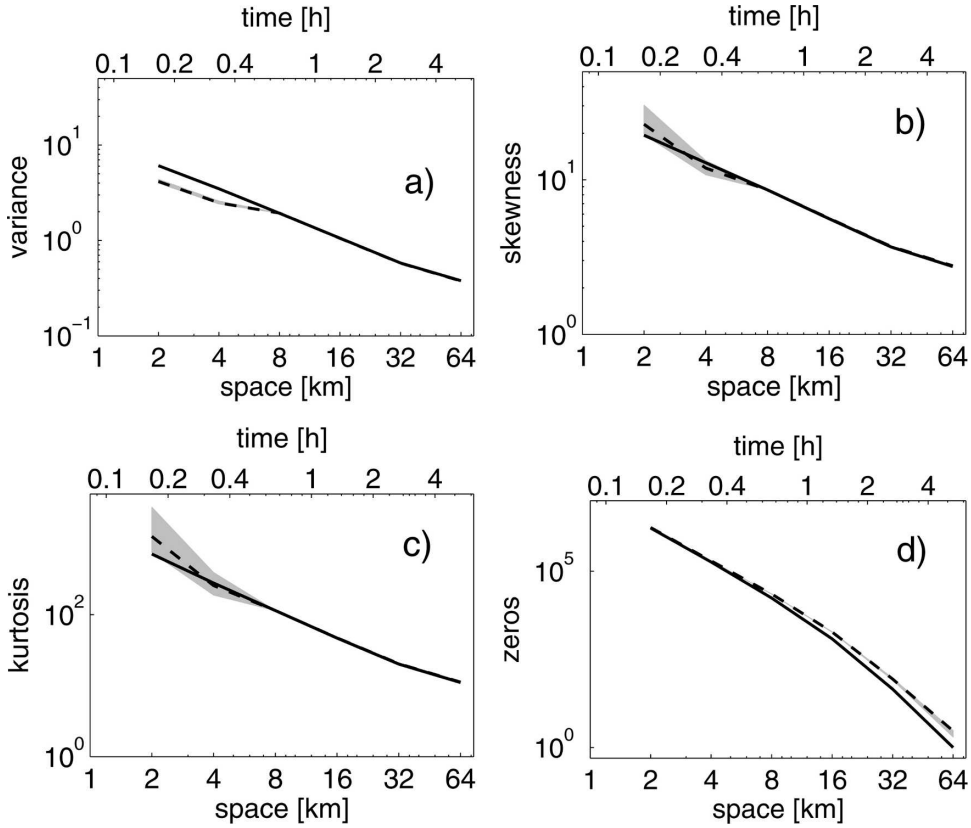

FIG. 8. Spatiotemporal scale dependence of the (a) variance, (b) skewness, (c) kurtosis, and (d) number of regions with zero precipitation for the original and for an ensemble of 100 realizations of RainFARM fields for the TOGA COARE event. A small threshold $r_0 = 0.2$ mm h^{-1} has been introduced at the smallest scales. Solid lines indicate the moments of the original fields, dashed lines indicate the average on the ensemble of stochastic realizations, and the shaded gray area includes 95% of the moments of the downscaled fields. Lower and upper horizontal scales indicate the spatial and temporal scales on which the average has been taken.

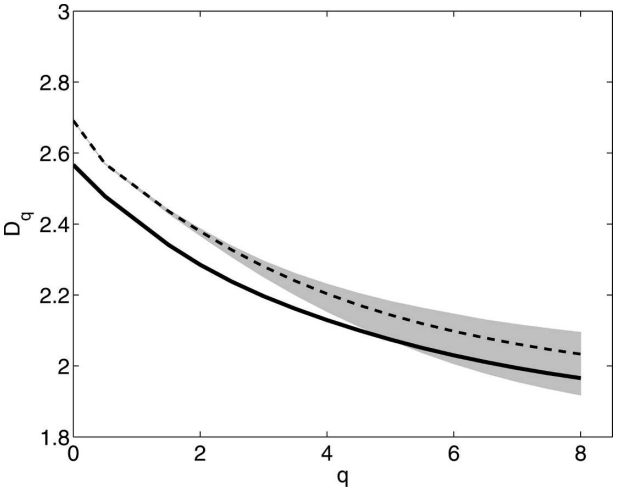

FIG. 9. Effective generalized fractal dimensions for the original field and for an ensemble of 100 realizations of RainFARM for the TOGA COARE event. The solid line indicates the generalized dimensions of the original field, the dashed line indicates the average on the ensemble of stochastic realizations, and the shaded gray area includes 95% of the dimensions of the downscaled fields. The generalized dimensions have been estimated from the average logarithmic slopes of the partition functions in the scale range from (4 km, 20 min) to (64 km, 320 min).

To this end, we consider an intense rainfall event forecasted by the ARPA SIM version of the Lokal Modell (Doms and Schattler 1998) over northwestern Italy. The forecasted event took place on 30 October 2004, starting at 0000 UTC, and it had a total duration of 42 h. The downscaling domain is a square area of 448-km sides that contains the Liguria, Lombardia, Piemonte, and Valle d'Aosta regions in Italy. The predicted LAM field has a spatial resolution of 7 km × 7 km and a time resolution of 3 h, and we generate downscaled fields with resolution of 1.75 km × 1.75 km in space and 11.25 min in time. We preserve the large-scale structure of the precipitation event predicted by the meteorological model, and we generate small-scale stochastic fields that are consistent with the LAM forecast in terms of rainfall volume and spectral properties.

Because of the fact that LAM precipitation forecasts are not reliable down to the numerical resolution scale, in the application of the downscaling procedure we define three scale regimes, namely,

- reliable scales: $L > L_0 = 28$ km, $T > T_0 = 12$ h, where we fully preserve the precipitation field provided by the model;
- unreliable scales: 7 km $< \lambda <$ 28 km, 3h $< \tau <$ 12 h, where the precipitation forecast provided by the LAM is considered to be unreliable (The choice of the "reliability scale" is somewhat arbitrary; here we adopt the standard choice of fixing the reliability scales at about 4 times the numerical resolution. Further work on the determination of reliability scales is needed; here we simply use the LAM field to provide an example of how the RainFARM can be implemented and we do not explore this problem further.); and
- unresolved scales: 1.75 km $< \lambda <$ 7 km, 11.25 min $< \tau <$ 3 h.

Thus, we start from a precipitation forecast defined on the spatial scales 28 km $\leq L \leq$ 448 km and temporal scales 12 h $\leq$ T $\leq$ 42 h, and we generate statistically downscaled fields that have spatial resolution $\lambda_0 = 1.75$ km and temporal resolution $\tau_0 = 11.25$ min.

Figure 10 shows one snapshot of the field predicted by the LAM and one of a downscaled field extracted from the ensemble produced by RainFARM (note the different spatial and temporal resolution of the two fields). The downscaled field has much stronger peaks of precipitation intensity, but it conserves the large-scale structure of the LAM forecast.

Figure 11 shows the spatial and temporal power spec-

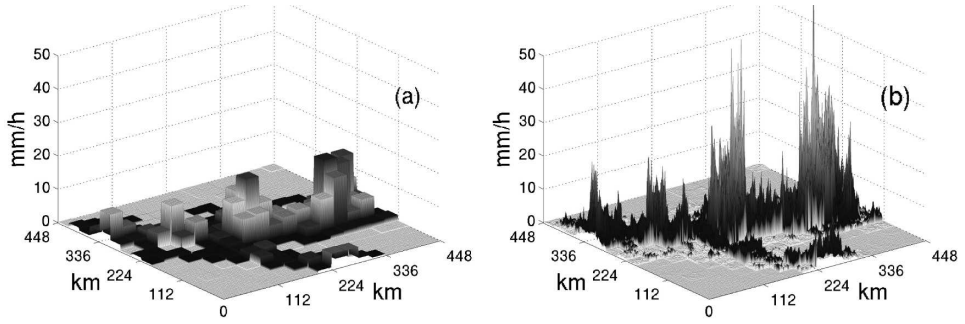

FIG. 10. (a) A snapshot of the forecasted rain field obtained from the LAM forecast and (b) one example of a downscaled field obtained by application of the RainFARM. The vertical scale indicates precipitation intensity (mm h^{-1}) and it is the same for the two fields.

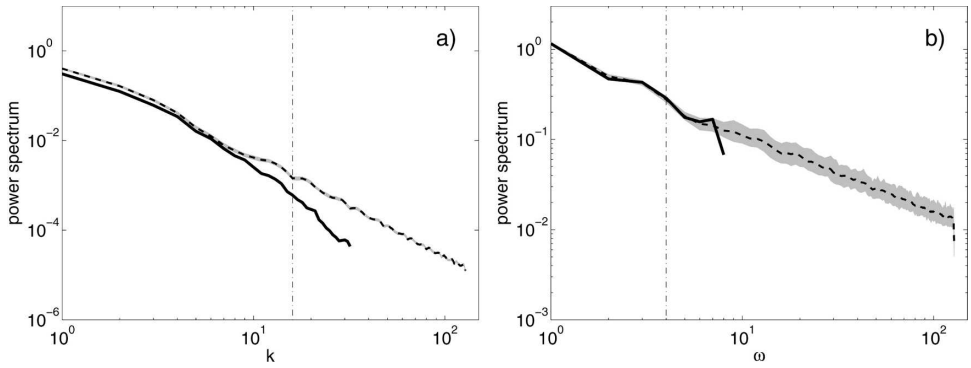

FIG. 11. (a) Spatial radial power spectrum and (b) temporal power spectrum of the original field and of an ensemble of 100 realizations of the stochastic field produced by RainFARM for the intense rainfall event predicted by the limited-area meteorological model discussed in the text. Solid lines indicate the spectra of the original fields, dashed lines indicate the average spectra on the ensemble of stochastic realizations, and the shaded gray area includes 95% of the spectra of the downscaled fields. The vertical dash-dotted line indicates the LAM "reliability scale" below which the downscaling procedure is applied.

tra of the original LAM field and of the ensemble of 100 downscaled fields. The spectra of the downscaled fields smoothly extrapolate the spectral information provided by the meteorological model.

Figure 12 shows the variance, skewness, and kurtosis of the original precipitation field and of the ensemble of RainFARM fields. The downscaling procedure has produced fields with the same total rainfall volume (by construction) but with much larger variance, skewness, and kurtosis, generating small-scale variability that was obviously absent in the original field.

Figure 13 shows the generalized fractal dimensions D_q versus the moment order q. A well-defined multifractal field is generated, similarly to what is observed for the radar data of the midlatitude precipitation event.

The example reported here shows how the RainFARM procedure can be applied to a real precipitation forecast provided by a LAM, and demonstrates what type of small-scale fields are to be expected. We are currently testing the performance of RainFARM by comparing the basin response from a rainfall-runoff model forced by high-resolution numerical weather forecasts and by an ensemble of downscaled fields obtained from the downscaling of a coarse-resolution version of the meteorological forecast. The results will be reported in a forthcoming manuscript.

6. Discussion and conclusions

In this work we have introduced a rainfall downscaling procedure that uses the information provided by meteorological models to generate stochastic precipitation fields with correct small-scale statistical properties. This procedure, called RainFARM, is based on the nonlinear transformation of a Gaussian random field and it produces non-Gaussian stochastic fields with the appropriate multifractal behavior. The repeated use of the downscaling procedure allows for generating an ensemble of high-resolution precipitation fields with given large-scale properties and correct small-scale statistics, to be used as an input to rainfall-runoff models for flood risk assessment (Siccardi et al. 2004).

Compared with other downscaling algorithms, the RainFARM procedure has the advantage that it includes the full conservation of the information provided by the LAM, which is a property that allows for maintaining the spatial and temporal localization of the rainfall patterns at larger scales.

The performance of the RainFARM procedure has been tested on two radar precipitation datasets, obtained during an intense rainfall event in central Italy and during TOGA COARE. We have aggregated the radar data to obtain coarse-grained fields with a resolution comparable to that of the rainfall predictions produced by limited-area meteorological models, and we have used the aggregated field as an input to the downscaling procedure. The reconstructed fields generated by RainFARM have then been compared with the original, high-resolution fields measured by radar. The comparison has shown that the downscaling procedure discussed here is able to generate fields that are very close, in terms of statistical properties, to the original fields. As an illustration of how RainFARM can be implemented in practice, we have applied the whole procedure to a LAM precipitation forecast of an intense rainfall event in Italy. In this paper, we have chosen specific functional forms for the power spectrum

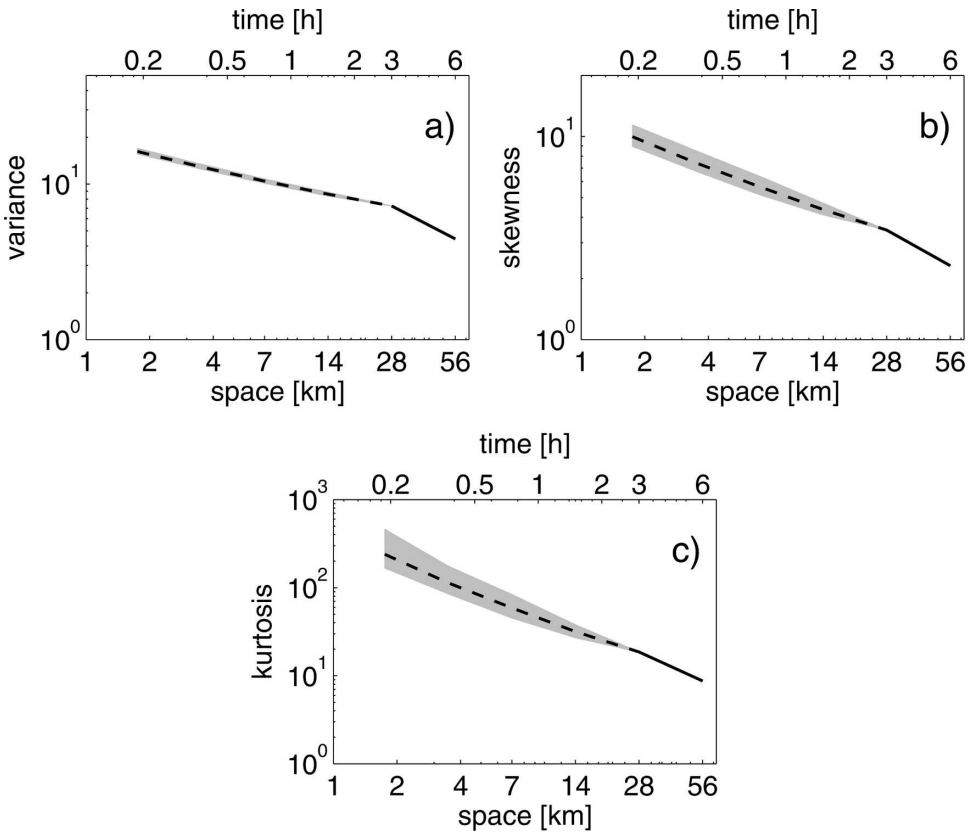

FIG. 12. Spatiotemporal scale dependence of the (a) variance, (b) skewness, and (c) kurtosis for the original and for an ensemble of 100 realizations of RainFARM fields for the intense midlatitude rainfall event predicted by the LAM. Solid lines indicate the moments of the original fields, dashed lines indicate the average on the ensemble of stochastic realizations, and the shaded gray area includes 95% of the moments of the downscaled fields. Lower and upper horizontal scales indicate the spatial and temporal scales on which the average has been taken.

and the nonlinear transformation used to generate the small-scale random fields. Other forms can easily be tested, using the same type of approach introduced here.

In the RainFARM procedure, the parameters used to generate the small-scale fields are estimated only from the knowledge of the rainfall fields to be downscaled. If the precipitation fields do not possess any approximate scaling, then it becomes difficult to downscale the information they provide. The examples considered here, however, indicate that a disaggregation procedure is possible. One should also be aware that the wider the range of scales reliably resolved in the original field, the better the estimates of the model parameters. If the rainfall field to be downscaled has low spatial and/or temporal resolution and it is recorded on a short interval of time, it may become difficult to correctly estimate the spectral slopes. In such cases, it may be preferable to use previously tabulated values that refer to various types of synoptic conditions (e.g., frontal precipitation, convective events, etc.).

Since the downscaling approach is based on extrapolating the information provided by the LAM, the whole procedure is sensitive to errors in the meteorological model. If the LAM has produced a wrong forecast, then the downscaling procedure cannot correct it. One further option is to apply the RainFARM procedure to an ensemble of limited-area meteorological forecasts (Molteni et al. 2001). In this case, we obtain an ensemble of stochastic fields for each member of the ensemble of meteorological predictions and take advantage of the better performances of ensemble prediction systems.

The implementation of the RainFARM approach is straightforward and the algorithm runs fast on any medium-sized workstation. For this reason, the procedure is easy to implement in operational chains for rainfall prediction and flood risk assessment. We are currently

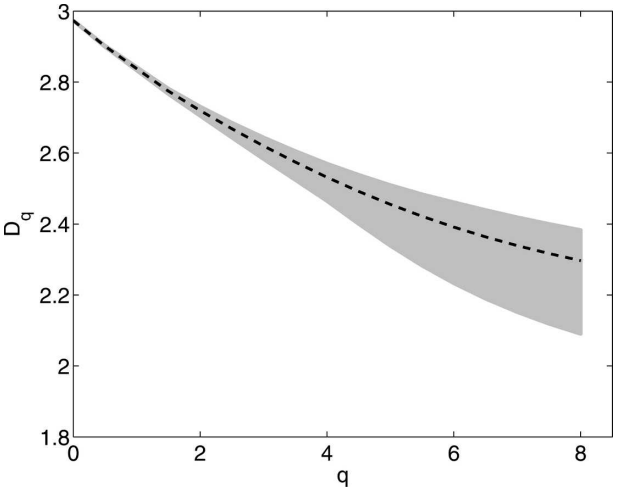

FIG. 13. Effective generalized fractal dimensions for an ensemble of realizations of RainFARM for the intense midlatitude event predicted by the LAM. The dashed line indicates the average on the ensemble of stochastic realizations, and the shaded gray area includes 95% of the dimensions of the downscaled fields. The generalized dimensions have been estimated from the average logarithmic slopes of the partition functions in the scale range from (3.5 km, 22.5 min) to (56 km, 6 h).

implementing RainFARM in one such operational framework in Italy. This will allow for continuous monitoring of the performance of the downscaling procedure under different types of meteorological conditions.

Acknowledgments. We thank Pierpaolo Alberoni of ARPA-SIM, Emilia Romagna, Italy, for providing the midlatitude radar data, Kerry Emanuel and Roberto Deidda for many interesting discussions, and Franco Siccardi for insightful comments. The comments of two anonymous referees on a previous version of this work greatly helped to improve our approach. This work was funded by the CNR-GNDCI project RAM, "Ricerca Applicata in Meteoidrologia," and the National Civil Protection of Italy.

REFERENCES

Adlerman, E., and K. Drogemeier, 2002: The sensitivity of numerically simulated cyclic mesocyclogenesis to variations in model physical and computational parameters. *Mon. Wea. Rev.,* **130,** 2671–2691.

Balmforth, N. J., A. Provenzale, E. A. Spiegel, M. Martens, C. Tresser, and C. W. Wu, 1999: Red spectra from white and blue noise. *Proc. Roy. Soc.,* **266B,** 311–314.

Bell, T. L., 1987: A space–time stochastic model of rainfall for satellite remote sensing studies. *J. Geophys. Res.,* **92** (D8), 9631–9643.

Cowpertwait, P. S. P., C. G. Kilsby, and P. E. O'Connell, 2002: A space-time Neyman-Scott model of rainfall: Empirical analysis of extremes. *Water Resour. Res.,* **38,** 1131, doi:10.1029/2001WR000709.

Davis, A., A. Marshak, W. Wiscombe, and R. Cahalan, 1994: Multifractal characterization of nonstationarity and intermittency in geophysical fields: Observed, retrieved, or simulated. *J. Geophys. Res.,* **99** (D4), 8055–8072.

Deidda, R., 2000: Rainfall downscaling in a space-time multifractal framework. *Water Resour. Res.,* **36,** 1779–1794.

——, R. Benzi, and F. Siccardi, 1999: Multifractal modeling of anomalous scaling laws in rainfall. *Water Resour. Res.,* **35,** 1853–1867.

——, M. G. Badas, and E. Piga, 2004: Space-time scaling in high-intensity Tropical Ocean Global Atmosphere Coupled Ocean-Atmosphere Response Experiment (TOGA-COARE) storms. *Water Resour. Res.,* **40,** W02506, doi:10.1029/2003WR002574.

Doms, G., and U. Schattler, 1998: The non-hydrostatic limited area model LM (Lokal Model) of DWD. Part I. Scientific documentation. Deutscher Wetterdienst, 160 pp. [Available online at http://cosmo-model.cscs.ch.]

Eagleson, P. S., N. M. Fenessey, W. E. Quiliang, and I. Rodriguez-Iturbe, 1987: Application of spatial Poisson models to airmass thunderstorm rainfall. *J. Geophys. Res.,* **92** (D8), 9961–9978.

Ferraris, L., R. Rudari, and F. Siccardi, 2002: The uncertainty in the prediction of flash floods in the northern mediterranean environment. *J. Hydrometeor.,* **3,** 714–727.

——, S. Gabellani, U. Parodi, N. Rebora, J. von Hardenberg, and A. Provenzale, 2003a: Revisiting multifractality in rainfall fields. *J. Hydrometeor.,* **4,** 544–551.

——, ——, N. Rebora, and A. Provenzale, 2003b: A comparison of stochastic models for spatial rainfall downscaling. *Water Resour. Res.,* **39,** 1368–1384.

Guillot, G., and T. Lebel, 1999: Disaggregation of Sahelian mesoscale convective system rain fields: Further developments and validation. *J. Geophys. Res.,* **104,** 31 533–31 551.

Gupta, V. K., and E. C. Waymire, 1993: A statistical analysis of mesoscale rainfall as a random cascade. *J. Appl. Meteor.,* **32,** 251–267.

Houze, R. A., Jr., 1977: Radar characteristic of tropical convection observed during GATE. *Mon. Wea. Rev.,* **105,** 964–980.

——, and A. K. Betts, 1981: Convection in GATE. *Rev. Geophys.,* **19,** 541–576.

Kumar, P., and E. Foufoula-Georgiou, 1993a: A multicomponent decomposition of spatial rainfall fields: 1. Segregation of large-scale and small-scale features using wavelet transforms. *Water Resour. Res.,* **29,** 2515–2532.

——, and ——, 1993b: A multicomponent decomposition of spatial rainfall fields: 2. Self-similarity in fluctuations. *Water Resour. Res.,* **29,** 2533–2544.

Lanza, L. G., 2000: A conditional simulation model of intermittent rain fields. *Hydrol. Earth Syst. Sci.,* **4,** 173–183.

Lovejoy, S., and B. Mandelbrot, 1985: Fractal properties of rain and a fractal model. *Tellus,* **37A,** 209–232.

Marani, M., 2005: Non power-law scale properties of rainfall in space and time. *Water Resour. Res.,* **41,** W08413, doi:10.1029/2004WR003822.

Mejia, J., and I. Rodriguez-Iturbe, 1974: On the synthesis of random fields sampling from the spectrum: An application to the generation of hydrologic spatial processes. *Water Resour. Res.,* **10,** 705–711.

Menabde, M., A. Seed, D. Harris, and G. Austin, 1997a: Self-similar random fields and rainfall simulations. *J. Geophys. Res.,* **102D,** 13 509–13 515.

——, D. Harris, A. Seed, G. Austin, and D. Stow, 1997b: Multiscaling properties of rainfall and bounded random cascades. *Water Resour. Res.,* **33,** 2823–2830.

——, A. Seed, G. Harris, and G. Austin, 1999: Multiaffine random field model of rainfall. *Water Resour. Res.,* **35,** 509–514.

Molteni, F., R. Buizza, C. Marsigli, A. Montani, F. Nerozzi, and T. Paccagnella, 2001: A strategy for high-resolution ensemble prediction. Part I: Definition of representative members and global model experiments. *Quart. J. Roy. Meteor. Soc.,* **127,** 2069–2094.

Northrop, P., 1998: A clustered spatial-temporal model of rainfall. *Proc. Roy. Soc. London,* **454A,** 1875–1888.

Over, T. M., and V. K. Gupta, 1994: Statistical analysis of mesoscale rainfall: Dependence of a random cascade generator on large-scale forcing. *J. Appl. Meteor.,* **33,** 1526–1542.

——, and ——, 1996: A space-time theory of mesoscale rainfall using random cascades. *J. Geophys. Res.,* **101** (D21), 26 319–26 331.

Perica, S., and E. Foufoula-Georgiou, 1996: Model for multiscale disaggregation of spatial rainfall based on coupling meteorological and scaling descriptions. *J. Geophys. Res.,* **101** (D21), 26 347–26 361.

Pielke, R. A., 1984: *Mesoscale Meteorological Modeling.* 2d ed. Academic Press, 750 pp.

Polyak, I., and G. North, 1995: The second-moment climatology of the GATE rain rate data. *Bull. Amer. Meteor. Soc.,* **76,** 535–550.

Rodriguez-Iturbe, I., D. R. Cox, and P. S. Eagleson, 1986: Spatial modelling of total storm rainfall. *Proc. Roy. Soc. London,* **403A,** 27–50.

Schertzer, D., and S. Lovejoy, 1987: Physical modeling and analysis of rain and clouds by anisotropic scaling multiplicative processes. *J. Geophys. Res.,* **92,** 9693–9714.

Schiesser, H. H., R. A. Houze Jr., and H. Huntrieser, 1995: The mesoscale structure of severe precipitation systems in Switzerland. *Mon. Wea. Rev.,* **123,** 2070–2097.

Short, D. A., P. A. Kucera, B. S. Ferrier, J. C. Gerlach, S. A. Rutledge, and O. W. Thiele, 1997: Shipboard radar rainfall patterns within the TOGA COARE IFA. *Bull. Amer. Meteor. Soc.,* **78,** 2817–2836.

Siccardi, F., G. Boni, L. Ferraris, R. Rudari, 2004: A hydrometeorological approach for probabilistic flood forecast. *J. Geophys. Res.,* **110,** D05101, doi:10.1029/2004JD005314.

Veneziano, D., and V. Iacobellis, 2002: Multiscaling pulse representation of temporal rainfall. *Water Resour. Res.,* **38,** 1138, doi:10.1029/2001WR000522.

——, R. L. Bras, and J. D. Niemann, 1996: Nonlinearity and self-similarity of rainfall in time and a stochastic model. *J. Geophys. Res.,* **101D,** 26 371–26 392.

von Hardenberg, J., R. Thieberger, and A. Provenzale, 2000: A box-counting red herring. *Phys. Lett.,* **269A,** 303–308.

——, L. Ferraris, and A. Provenzale, 2003: The shape of convective rain cells. *Geophys. Res. Lett.,* **30,** 2280, doi:10.1029/2003GL018539.

Waymire, E. C., V. K. Gupta, and I. Rodriguez-Iturbe, 1984: A spectral theory of rainfall intensity at the meso-beta scale. *Water Resour. Res.,* **20,** 1483–1465.

Webster, P. J., and R. Lukas, 1992: TOGA-COARE: The Coupled Ocean-Atmosphere Response Experiment. *Bull. Amer. Meteor. Soc.,* **73,** 1377–1416.

Wheater, H. S., and Coauthors, 2000: Spatial-temporal rainfall fields: Modelling and statistical aspects. *Hydrol. Earth Syst. Sci.,* **4,** 581–601.

Willems, P., 2001: A spatial rainfall generator for small spatial scales. *J. Hydrol.,* **252,** 126–144.